

# Simulating X-ray Clusters with Adaptive Mesh Refinement

Greg L. Bryan

*Physics Department, MIT, Cambridge, MA 02139*

Michael L. Norman

*National Center for Supercomputing Applications; and  
Astronomy Department, University of Illinois at Urbana-Champaign,  
Urbana, IL 61801*

## Abstract.

Gravitational instabilities naturally give rise to multi-scale structure, which is difficult for traditional Eulerian hydrodynamic methods to accurately evolve. This can be circumvented by adaptively adding resolution (in the form of multiple levels of finer meshes) to relatively small volumes as required. We describe an application of this adaptive mesh refinement (AMR) technique to cosmology, focusing on the formation and evolution of X-ray clusters. A set of simulations are performed on a single cluster, varying the initial resolution and refinement criteria. We find that although new, small scale structure continues to appear as the resolution is increased, bulk properties and radial profiles appear to converge at an effective resolution of  $8192^3$ . We find good agreement with the “universal” dark matter profile of Navarro, Frenk & White (1995).

## 1. Introduction

Due to their high luminosity and relative simplicity, X-ray clusters provide one of the most precise measurements of the amplitude of mass fluctuations in our universe. Combined with the observed anisotropy of the cosmic background radiation, it serves as a key constraint on cosmological models (Henry et al. 1992; Eke, Cole & Frenk 1996). There are, however, a number of unresolved difficulties in our understanding of clusters. These include the refusal of clusters to agree with some analytic scaling laws (Edge & Stewart 1991a), a result which adiabatic simulations seem unable to explain (Navarro, Frenk & White 1995). Also, the apparent decrease in the number of X-ray clusters at high redshift (Castander et al. 1993; Bower et al. 1994) is unexpected in the context of many popular models as well as being discrepant with optical observations of rich, distant clusters (Couch et al. 1991; Postman 1993). Having fixed the number density of clusters at  $z = 0$ , the rate of evolution is a strong indicator of cosmology, especially with regard to the value of  $\Omega$ , thus it is important to better understand the structure and formation of X-ray clusters.

While N-body studies provide much useful information (Cole & Lacey 1996), clusters are observationally identified either through their galaxies or by X-ray emission from a hot gas component. Since galaxies are very difficult to model correctly, and do not provide as straightforward a tracer of clusters as X-ray observations, we turn to the baryonic gas. Most studies of individual X-ray clusters incorporating hydrodynamics have employed Lagrangian, particle-based methods (Evrard 1990; Katz & White 1993). Although these Smoothed Particle Hydrodynamics (SPH) methods provide excellent spatial resolution when combined with a suitable gravity solver, their shock-capturing capabilities are not as good as modern Eulerian methods. However, most cosmological Eulerian codes are hampered by a fixed grid and so provide good resolution in low-density regions, but poor resolution in high-density regions, such as the centers of X-ray clusters (Kang et al. 1994).

Here, we present first results from a new method which is designed to provide adaptive resolution combined with a shock-capturing Eulerian hydrodynamics scheme. This Adaptive Mesh Refinement (AMR) technique provides high resolution within small regions, the location of which are controlled automatically (Berger & Colella 1989). We use the piecewise parabolic method, adapted to cosmology (Bryan et al. 1995), for the baryons, particles for dark matter and a high-resolution gravity solver; however, due to space constraints, we defer discussion of the methodology to a future paper.

## 2. Results

We have simulated the formation of an adiabatic X-ray cluster in an  $\Omega = 1$  universe. The initial spectrum of density fluctuations is CDM-like with a shape parameter of  $\Gamma = 0.25$  (Efstathiou et al. 1992b); the cluster itself is a constrained  $3\text{-}\sigma$  fluctuation at the center, for a Gaussian filter of 10 Mpc. We use a Hubble constant of 50 km/s/Mpc and a baryon fraction of 10%. This cluster is the subject of a comparison project between twelve different simulation methods, the results of which will be presented in an upcoming paper (Frenk et al. 1996).

The simulation was initialized with two grids. The first is the root grid covering the entire  $64 \text{ Mpc}^3$  domain with  $64^3$  cells. The second grid is also  $64^3$  cells but is only 32 Mpc on a side and is centered on the cluster. Thus, over the region that forms the cluster, we have an initial cell size of 500 kpc leading to an approximate mass resolution of  $8.7 \times 10^8 M_\odot$  ( $7.8 \times 10^9 M_\odot$ ) for the baryons (dark matter). We adopt a refinement mass for the baryons of  $4M_{initial} \approx 3.5 \times 10^9 M_\odot$  (i.e. if the mass in any cell exceeds this value a finer mesh is created), but only allow refined grids within a box 25.6 Mpc on a side, centered on the cluster center since we are uninterested in objects outside this volume. Some objects will collapse outside this region and then move inside; these halos will not be properly modelled as high resolution is required throughout an object's evolution (Anninos & Norman 1996). We will focus mostly on the properties of the central cluster, which collapsed entirely within the refined region. We have also run a set of AMR simulations for the same cluster with lower mass resolution and initial power in order to examine numerical convergence.

In Figure 1, we show a typical example of the grid layout in this simulation. The top panel depicts the dark matter distribution in order to show the

collapsed structure. A projection of the level hierarchy is shown below, with grids colour-coded by level. We do not show the full three-dimensional layout since, with about 400 grids, this would be too complicated to extract much useful information; however, the grid ‘shadows’ do demonstrate that the grid structure mirrors the mass morphology. The range of grid sizes and shapes is diverse, but most tend to be in the range of 10–60 zones per edge and largely rectangular. The images are 32 Mpc on a side; note the unrefined region around the boundary of the figure. A side effect of the quasi-Lagrangian refinement criterion coupled with the varying cell size is that the *rms* density fluctuations are roughly constant (on a log basis) throughout the hierarchy. This means that the gravitational force errors due to shot noise from the finite number of particles is roughly independent of density, rather than rising sharply in low density regions as in traditional high-resolution gravity schemes, such as P<sup>3</sup>M and tree-codes.

Figure 2 shows the baryonic and dark matter density profiles for this cluster. In order to gauge the convergence, results from three other AMR runs are also plotted. These runs had smaller initial grids (16<sup>3</sup>, 32<sup>3</sup> and 64<sup>3</sup>) and therefore poorer mass resolution and less initial power. We also plot the profile from Navarro et al. (1996) for the dark matter,

$$\frac{\rho(r)}{\rho_{crit}} = \frac{\delta_0}{(r/r_s)(1+r/r_s)^2}, \quad (1)$$

where  $r_s = r_{vir}/c$  and  $\delta_0$  is set by the requirement that the mean density within the virial radius be 178 times the critical density. Setting the parameter  $c = 8$  produces a remarkably good fit over three orders of magnitude.

The gas density profile levels off at a few hundred kpc, around the knee in the dark matter profile. Lower resolution results exhibit systematically lower densities, and although we have not converged, the difference between the 64<sup>3</sup> initial grid and the higher-resolution run is slight. We remind the reader that this simulation does not include radiative cooling which would significantly affect the dynamics and structure of the inner few hundred kpc. The turnover in density agrees with that seen in entropy, shown in the same figure. There appears to be a cutoff in the entropy distribution, the cause of which is not currently understood.

### 3. Conclusion

The AMR algorithm is complementary to other simulation techniques, such as SPH and Eulerian single grid method. The advantage of AMR is that it provides higher resolution than Eulerian methods and better shock capturing features than SPH codes. Further, it is more flexible than Lagrangian codes because we can control where the resolution is placed by changing the refinement criterion. Also, since each level advances with its own timestep the entire computation does not have to proceed at the speed of its slowest component (some SPH codes also share this feature). The primary disadvantage is that the scheme is somewhat more complicated to code and modify; this implementation uses a combination of C++ to handle the dynamic grid hierarchy and FORTRAN 77 for computationally intensive tasks.

Here we have demonstrated that AMR can model an X-ray cluster with many of the same desirable characteristics of the single-grid code but with much

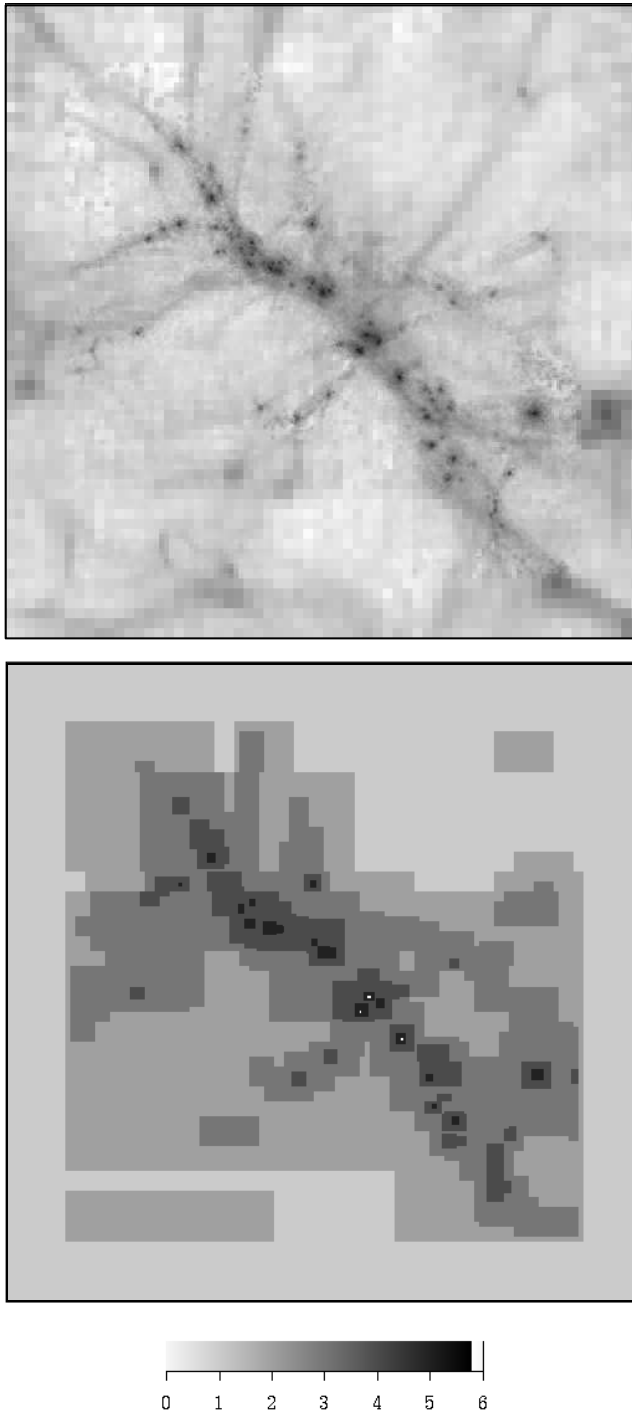


Figure 1. The logarithm of the dark matter surface density (top) and the projected grids (bottom), colour coded by level at  $z = 2$ . In order to increase the contrast of the three small level 6 grids, they have been coloured white. The figures are 32 Mpc on a side.

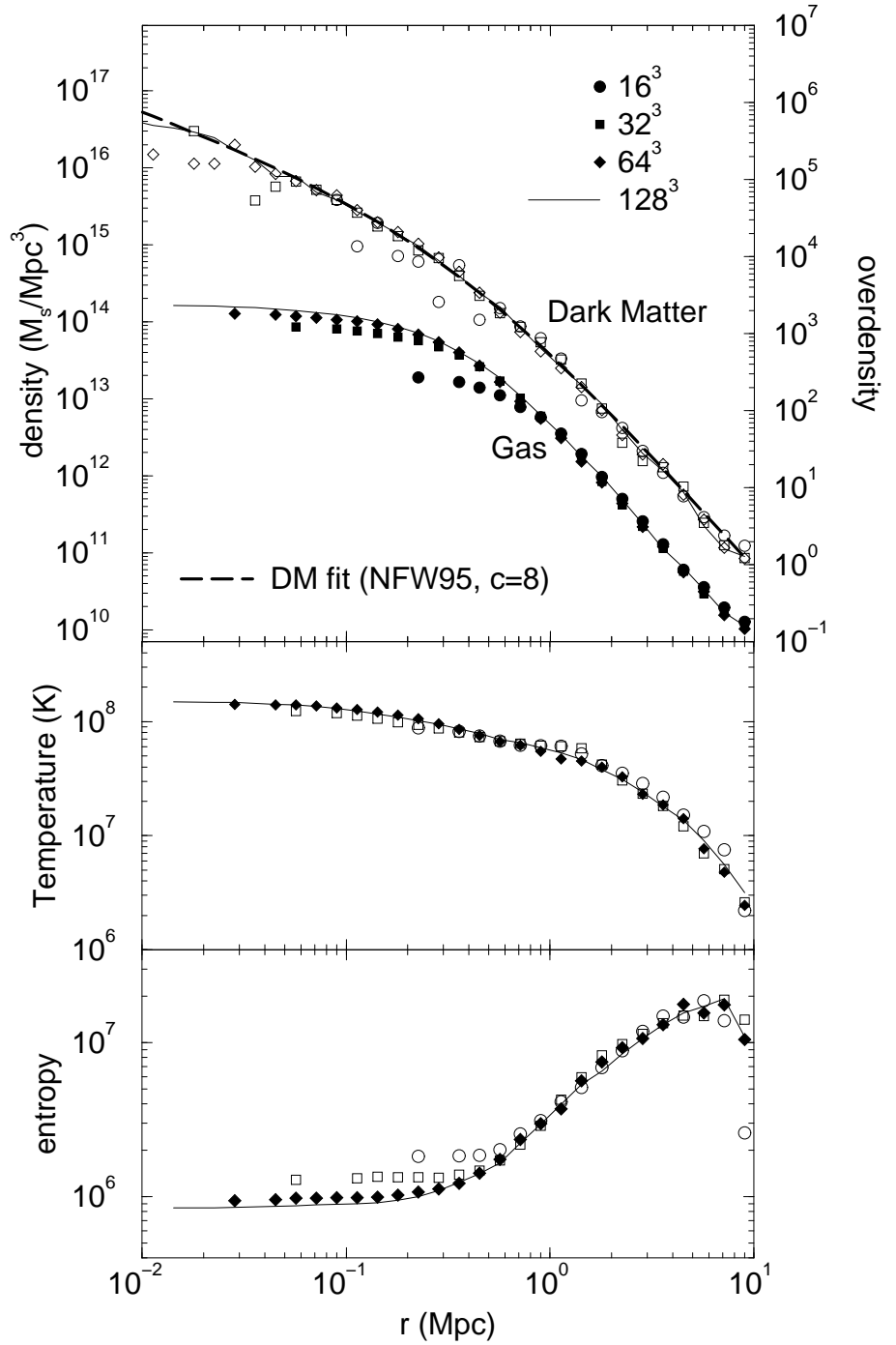


Figure 2. From top to bottom: i) Dark matter (top curve) and baryonic (bottom curve) radial density profiles, ii) temperature profile, iii) entropy profile. Four different runs are shown with varying initial grid sizes (which also roughly indicates the mass resolution):  $16^3$ ,  $32^3$ ,  $64^3$  and the effective  $128^3$  run. The solid dashed line overlaid the dark matter profile is the fit from equation 1.

higher resolution. The efficiency of the AMR method over a single grid for this simulation is quite high: a factor of 4000 in memory and 20 000 in CPU, although, of course, the resulting solution is not as good in low density regions.

**Acknowledgments.** We acknowledge useful discussions with Henry Neeman and Edmund Bertschinger. This work is done under the auspices of the Grand Challenge Cosmology Consortium and supported in part by NSF grants ASC-9318185 and NASA Long Term Astrophysics grant NAGW-3152.

## References

- Anninos, P. & Norman, M.L. 1996, *ApJ*, 459, 12
- Berger, M.J. & Colella, P. 1989, *J. Comput. Phys.*, 82, 64
- Bower, R.G., Böhringer, Brial, U.G., Ellis, R.S., Castander, F.J., & Couch, W.J. 1994, *MNRAS*, 268, 345
- Bryan, G.L., Norman, M.L., Stone J.M., Cen, R., Ostriker, J.P. 1995, *Comput. Phys. Comm.*, 89, 149
- Castander, F.J., Ellis, R., S., Frenk, C.S., Dressler, A. & Gunn, J.E. 1994, *ApJ*424, L79
- Cole, S. & Lacey, C. 1996, preprint (astro-ph/9510147)
- Colella, P. & Woodward, P.R. 1984, *J. Comput. Phys.*, 54, 174
- Couch, W.J., Ellis, R.S., Malin, D.F., & MacLaren, I. 1991, *MNRAS*, 249, 606
- Edge, A.C. & Stewart, G.C. 1991a, *MNRAS*, 252, 414
- Efstathiou, G., Dalton, G.B., Sutherland, W.J., Maddox S.J. 1992, *MNRAS*, 257, 125
- Eke, V.R., Cole, S., & Frenk, C.S. 1996, *MNRAS*, submitted
- Evrard, A.E. 1990, *ApJ*, 363, 349
- Frenk, C.S. et al. 1996, in preparation
- Henry, J.P., Gioia, I.M, Maccacaro, T., Morris, S.L., Stocke, J.T., & Wolter, A. 1992, *ApJ*, 386, 408
- Kang, H., Ostriker, J.P, Cen, R., Ryu, D., Hernquist, L., Evrard, A.E., Bryan, G.L., & Bryan, G.L. 1994, *ApJ*, 430, 80
- Katz, N., & White, S.D.M. 1993, *ApJ*, 412, 455
- Navarro, J.F., Frenk, C.S., White, S.D.M. 1995, *MNRAS*, 275, 720
- Navarro, J.F., Frenk, C.S., White, S.D.M. 1995, *ApJ*, 462, 563
- Postman, M. 1993, in *Observational Cosmology*, ASP Conf. Ser. 51, edited by G. Chincarini, A. Iovino, T. Maccacaro, and D. Maccagne (ASP, San Francisco), p. 260